

Template iterations of quadratic maps and hybrid Mandelbrot sets

Anca Rădulescu^{*,1}, Kelsey Butera¹, Brandee Williams¹

¹ Department of Mathematics, SUNY New Paltz, NY 12561

Abstract

As a particular problem within the field of non-autonomous discrete systems, we consider iterations of two quadratic maps $f_{c_0} = z^2 + c_0$ and $f_{c_1} = z^2 + c_1$, according to a prescribed binary sequence, which we call *template*. We study the asymptotic behavior of the critical orbits, and define the Mandelbrot set in this case as the locus for which these orbits are bounded. However, unlike in the case of single maps, this concept can be understood in several ways. For a fixed template, one may consider this locus as a subset of the parameter space in $(c_0, c_1) \in \mathbb{C}^2$; for fixed quadratic parameters, one may consider the set of templates which produce a bounded critical orbit. In this paper, we consider both situations, as well as *hybrid* combinations of them, we study basic topological properties of these sets and propose applications.

Using random iterations of discrete functions, we build a mathematical framework that can be used to study the effect of errors in copying mechanisms (such as DNA replication). In our theoretical setup – in which one of the functions is the correct one, and the other one is the erroneous perturbation – we consider problems that a sustainable replication system may have to solve when facing the potential for errors. We find that it is possible to tell which specific errors are more likely to affect the system’s dynamics, in absence of prior knowledge of their timing. Moreover, within an optimal locus for the correct function, almost no errors can affect the sustainability of the system. Mathematically, our work complements broader existing results in non-autonomous dynamics with more specific detail for the case of two random iterated functions, which is a valuable context for applications.

1 Introduction

For iterations of single complex maps, the Julia set is defined as the boundary (in the complex plane) between initial conditions which remain asymptotically bounded and those which escape to infinity under iterations of the map. The topological and fractal properties of Julia sets have been most studied for polynomials, with major results relating the geometry of the Julia set with properties of the critical orbits. In particular, for iterations of single quadratic maps in the family $f_c = z^2 + c$, with $c \in \mathbb{C}$, the Julia set is either connected, if the orbit of the critical point 0 is bounded, or totally disconnected, if the orbit of the critical point 0 is unbounded.

While quadratic iterations have been often used to represent natural phenomena, it is unlikely that natural systems evolve according to the same identical dynamics along time. A more realistic mathematical framework to model the variability and errors that appear in replication systems is that of time-dependent (non-autonomous) iterations, in which the iterated map may change between steps (evolve in time). Random iterations have been studied since the early 1990’s, starting with the work of Fornaess and Sibony [7]. More recent work has focused on the asymptotic dynamics of non-autonomous systems, and on defining extensions of the Julia and Mandelbrot set in the context of random iterations [8, 9, 10]. The simple particular case of an iteration which alternates two distinct quadratic complex maps (thus equivalent to iterating a complex quartic polynomial) was studied by Danca et al. [11]. It was shown that in this case the Julia sets can be disconnected without being totally disconnected, and that they exhibit graphical alternation.

¹Assistant Professor, Department of Mathematics, State University of New York at New Paltz; New York, USA; Phone: (845) 257-3532; Email: radulesa@newpaltz.edu

As in our previous work [12], we consider here iterations of two different functions, f_{c_0} and f_{c_1} , according to a general binary symbolic sequence \mathbf{s} (*template*), in which the “zero” positions correspond to iterating the function f_{c_0} and the “one” positions correspond to iterating the function f_{c_1} . We view template iterations as a more appropriate framework for replication or learning algorithms that appear in nature, with patterns that evolve in time, and which may involve occasional, random or periodic “errors.” While our results generally agree with existing results in non-autonomous iterations, our interest resides more specifically in understanding the dependence of the dynamic behavior on the two primary features of this system’s hardwiring: (1) the complex parameter pair (c_0, c_1) that fixes the iterated maps and (2) the structure of the template, i.e. the particular succession (timing) of the 0s and 1s that govern the iteration order.

Broadly speaking, one can interpret iterated orbits as describing the temporal trajectories of an evolving system (e.g., DNA replication algorithm, or learning neural network). Along these lines, an initial condition which escapes to ∞ under iterations (i.e., a point in the Fatou set) may be seen as a feature of the system which becomes unsustainable in time, while an initial condition which is promptly attracted to a simple periodic orbit (i.e., a point in the interior of the Julia set) may represent a feature which is too simple to be relevant to the system. Then the points on the boundary between these two behaviors (i.e., the Julia set) may be viewed as the set of optimal features, allowing the system to operate in a dynamic regime ideal for performing its complex function. One can study how the “sustainable set of features” (filled Julia set) changes when introducing occasional or periodic errors into the iteration process. For example, investigating the types of errors for which the Julia set is disconnected would help identify the systems capable of functioning in a sustainable range, when they are initiated within multiple connected loci of initial conditions [12].

In our previous work, we noticed that all maps in the quadratic family have the same critical point $\xi_0 = 0$, which we identified as the system’s “resting state.” By analogy with the traditional case of single quadratic map iterations (studied by Benoit Mandelbrot), and in order to promote applications to natural systems, we defined the Mandelbrot set under template iterations as the parameter locus for which the critical point remains bounded (that is, the system evolves along a functionally sustainable trajectory when iterated from rest). More precisely, for a fixed $(c_0, c_1, \mathbf{s}) \in \mathbb{C}^2 \times \{0, 1\}^\infty$, we study the iterated orbit:

$$\xi_0 = 0 \rightarrow f_{c_{s_1}}(0) \rightarrow (f_{c_{s_2}} \circ f_{c_{s_1}})(0) \rightarrow \cdots \rightarrow (f_{c_{s_n}} \circ \cdots \circ f_{c_{s_1}})(0) \rightarrow \cdots$$

When $c_0 = c_1$, the orbit does not depend on \mathbf{s} and corresponds to the traditional orbit of ξ_0 under the quadratic polynomial $f_{c_0} = f_{c_1}$. In this slice, the Mandelbrot set is defined as the locus of all c_0 for which the orbit of the origin is bounded, or equivalently for which the Julia set of f_{c_0} is connected. Here, we extend the concept of Mandelbrot set to different slices of $\mathbb{C}^2 \times \{0, 1\}^\infty$, in which the two traditional definitions are no longer equivalent. In the scenario where an “erroneous” function f_{c_1} interferes into the iteration of a correct function f_{c_0} , one natural question to ask is how far can the erroneous map c_1 stray from the given correct map c_0 , so that we can be sure (with some probability) that the critical orbit $o_{\mathbf{s}}(0)$ stays bounded when a random template \mathbf{s} prescribes where the errors will hit in the iteration process. This is one of the questions which we address and illustrate in this paper.

A different possibility, raised previously by Comerford [8], is to consider the parameter locus for which the iteration is post-critically bounded. In our case, this means that none of the critical points $\xi_0 = 0$ introduced at any step $m \geq 1$ of the iteration, can escape to infinity. In other words, all orbits:

$$0 \rightarrow f_{c_{s_m}}(0) \rightarrow \cdots \rightarrow (f_{c_{s_n}} \circ \cdots \circ f_{c_{s_m}})(0) \rightarrow \cdots$$

are bounded.

In this paper, we first investigate the parameter locus for which only the orbit of the original critical point is requested to remain bounded. We consider how this definition applies in c_1 -parameter

slices \mathbb{C} , for fixed c_0 and \mathbf{s} , as well as in template slices in $\{0, 1\}^\infty$, for fixed pairs $(c_0, c_1) \in \mathbb{C}^2$. For these sets, as well as for hybrid combinations, we discuss topological properties of potential importance (such as connectivity), and we explore connections with other possible definitions. We then consider the stricter definition, for the iteration to be postcritically bounded in the sense described by Comerford and others, we investigate the same questions and compare the results. We discuss, for both definitions, the relationship of the Mandelbrot set with the connectedness locus of the Julia set for template iterations.

In our previous work, we introduced the *fixed template Mandelbrot set* [12] as the locus in \mathbb{C}^2 of (c_0, c_1) for which the critical orbit is bounded under a fixed template \mathbf{s} . We investigated some of the properties of this set and of its 2-dimensional complex slices for both periodic and random templates. For example, we suggested that there are detectable differences in the Hausdorff dimension along the boundary of Mandelbrot slices for fixed templates, between the case of periodic and that of non-periodic templates. Here we concentrate on fixing the complex parameter pair (c_0, c_1) , and understanding the topology of the *fixed-map* Mandelbrot defined as a Mandelbrot slice in the template space $\{0, 1\}^\infty$.

We then define *hybrid* Mandelbrot sets so that, for a fixed c_0 , they illustrate for all c_1 the likelihood of a random template to produce a bounded critical orbit $o_{\mathbf{s}}(0)$ under iterations of f_{c_0} and f_{c_1} . We find that the level sets of hybrids have a less complex geometric structure than the traditional Mandelbrot set, possibly relating to a known phenomenon of cooperation between generating maps towards “smoothing out the chaos” [10].

1.1 The quadratic family and template iterations

We will be working within the complex quadratic family

$$\{f_c: \mathbb{C} \rightarrow \mathbb{C} / f_c(z) = z^2 + c, \text{ with } c \in \mathbb{C}\}$$

For fixed parameters $c_0, c_1 \in \mathbb{C}$, and a fixed binary sequence $\mathbf{s} = (s_n)_{n \geq 0} \in \{0, 1\}^\infty$, one can define the template orbit for any $\xi_0 \in \mathbb{C}$ as the sequence $o_{\mathbf{s}}(\xi_0) = (\xi_n)_{n \geq 0}$ constructed recursively, for every $n \geq 0$, as:

$$\xi_{n+1} = f_{c_{s_n}}(\xi_n)$$

The parameter space of our template iterated system is $\mathbb{C}^2 \times \{0, 1\}^\infty$, with the quadratic parameter pair $(c_0, c_1) \in \mathbb{C}^2$, and the template $\mathbf{s} \in \{0, 1\}^\infty$. We defined two main types of “Mandelbrot” sets, in different slices of this parameter space [12].

Definition 1.1. Fix $\mathbf{s} \in \{0, 1\}^\infty$ a symbolic sequence. The corresponding *fixed-template Mandelbrot set* is defined as:

$$\mathcal{M}_{\mathbf{s}} = \{(c_0, c_1) \in \mathbb{C}^2, \text{ where } o_{\mathbf{s}}(0) \text{ is bounded} \}$$

Definition 1.2. Fix $(c_0, c_1) \in \mathbb{C}^2$. The corresponding *fixed-map Mandelbrot set* is defined as:

$$\mathcal{M}_{c_0, c_1} = \{\mathbf{s} \in \{0, 1\}^\infty, \text{ where } o_{\mathbf{s}}(0) \text{ is bounded} \}$$

One may consider each template $\mathbf{s} \in \{0, 1\}^\infty$ as corresponding to the binary expansion of a number $a_{\mathbf{s}} \in [0, 1]$. Then a fixed-map Mandelbrot set \mathcal{M}_{c_0, c_1} can be viewed as the subset of all $a_{\mathbf{s}} \in [0, 1]$ for which the template orbit $o_{\mathbf{s}}(0)$ under (c_0, c_1) is bounded. We can then define a mixed, or *hybrid* Mandelbrot set, potentially related to phenomena of averaging out chaos, as described by Sumi in the context of non-autonomous iterations on polynomial semigroups [10].

Definition 1.3. Fix $c_0 \in \mathbb{C}$. The corresponding **hybrid Mandelbrot set** is defined as:

$$\mathcal{M}_{c_0} = \{(c_1, b) \in \mathbb{C} \times [0, 1], \text{ with } b = \mathcal{L}(\mathcal{M}_{c_0, c_1})\}$$

where \mathcal{L} designates the Lebesgue measure on the interval $[0, 1]$.

While in previous work we focused on fixed-template Mandelbrot sets, in the current paper we will investigate fixed-map and hybrid sets. The main goal of this paper is to visualize the structure and conjecture properties of these sets, in particular understand their dependence on the complex parameters and on the template structure, whichever appropriate in each case.

1.2 Escape radius for template iterations

A simple, yet major result in the case of iterations of single quadratic complex maps is the existence of escape radius [13]. More precisely:

Theorem 1.4. For any value of the parameter c , the critical orbit $(z_n)_n$ (for $z_0 = 0$) under the function $f_c(z) = z^2 + c$ has the escape radius $R_e = 2$. That is, if $|z_N| > 2$ for some positive integer N , then $|z_n| > 2$ for all $n \geq N$, and $|z_n| \rightarrow \infty$ as $n \rightarrow \infty$.

More general results have been formulated by Comerford et al. for the case of random iterations [8], as follows: Suppose we take $d \geq 2$, $K \geq 1$, $M \geq 0$ and let $(P_m)_{m=1}^\infty$ be a bounded sequence of polynomials, that is: (1) the degree d_m of each P_m satisfies $2 \leq d_m \leq d$; (2) the leading coefficients a_m satisfy $1/K \leq a_m \leq K$; (3) all coefficients of all P_m are within the disc of radius M . Then there exists $R > 0$ escape radius for the sequence P_m , that is: for all $m \geq 0$ and all $|z| \geq R$, we have $|P_n \circ \dots \circ P_{m+2} \circ P_{m+1}(z)| \rightarrow \infty$ as $n \rightarrow \infty$. Comerford et al. [8] showed that one can find an escape radius R which depends only on the bounds d , K and M , and works for every sequence which satisfies these bounds.

The existence and the value of the escape radius will be used in this study to determine numerically which orbits are unbounded, allowing elimination from the Mandelbrot set of the parameters for which the critical point iterates out of the escape radius. While Comerford's result permits custom computation of R_e for a general sequence of bounded polynomials, when iterating two quadratic maps according to a template, the escape rate is more reminiscent of single map iterations, so that $R_e = 2$ still acts as escape radius under some relatively broad assumptions. As a result tailored for template iterations, we have the following lemma:

Lemma 1.5. For arbitrary $(c_0, c_1, \mathbf{s}) \in \mathbb{C}^2 \times \{0, 1\}^\infty$, consider a template orbit $(\xi_n)_n$. Suppose $|\xi_N| > \max\{2, |c_0|, |c_1|\}$ for some N . Then $|\xi_n| > 2$ for all $n \geq N$, and $|\xi_n| \rightarrow \infty$ as $n \rightarrow \infty$.

Proof of lemma. Suppose $|\xi_n| > 2$ for some $n \geq N$ and calculate:

$$\frac{|\xi_{n+1}|}{|\xi_n|} = \frac{|f_{c_{s_n}}(\xi_n)|}{|\xi_n|} = \frac{|\xi_n^2 + c_{s_n}|}{|\xi_n|} \geq \frac{|\xi_n|^2 - |c_{s_n}|}{|\xi_n|} = |\xi_n| - \frac{|c_{s_n}|}{|\xi_n|}$$

Since $|\xi_n| > |c_{s_n}|$ for all n , the right side $|\xi_n| - \frac{|c_{s_n}|}{|\xi_n|} > |\xi_n| - 1$. Since $|\xi_n| > 2$, we further have:

$$\frac{|\xi_{n+1}|}{|\xi_n|} > |\xi_n| - 1 > 1$$

Since $|\xi_N| > 2$, this implies by induction that $|\xi_n| > 2$ for all $n \geq N$. In addition, we have $|\xi_{n+1}| > |\xi_n|$ for $n \geq N$, implying that the orbit converges in radius to its upper bound. If we assume that this upper bound is a finite number $l = \lim_{n \rightarrow \infty} |\xi_n|$, we get, taking limit on both sides of

$\frac{|\xi_{n+1}|}{|\xi_n|} \geq |\xi_n| - 1$, that the limit $l \leq 2$, which contradicts the fact that l is the upper bound of a sequence of values larger than 2. It follows that the limit $\lim_{n \rightarrow \infty} |\xi_n| = \infty$. \square

The lemma provides a direct and simple expression for the escape radius:

Theorem 1.6. *A template iteration of the maps c_0 and c_1 has escape radius $R_e = \max\{2, |c_0|, |c_1|\}$.*

This immediately implies that the escape radius of the critical orbit is $R_e = 2$ (as in the traditional case) under some additional conditions.

Proposition 1.7. *For fixed $c_0 = 0$ and any value of the parameter $c_1 \in \mathbb{C}$, the template orbit $(\xi_n)_n$ of $\xi_0 = 0$ under $(0, c_1)$ has escape radius $R_e = 2$. That is, if $|\xi_N| > 2$ for some positive integer N , then $|\xi_n| > 2$ for all $n \geq N$, and $|\xi_n| \rightarrow \infty$ as $n \rightarrow \infty$.*

Proof. Suppose first that $|c_1| \leq 2$. From $|\xi_N| > 2$, it follows automatically in this case that $|\xi_n| > \max\{2, |c_0|, |c_1|\}$. From Lemma 1.5, it further follows that $|\xi_n| > 2$ for all $n \geq N$, and $|\xi_n| \rightarrow \infty$ as $n \rightarrow \infty$.

Now we consider the case $|c_1| > 2$. We aim to track down when the critical orbit $o_s(0)$ leaves the disk of radius 2. The orbit will remain zero as long as the map f_{c_0} is iterated, that is throughout the first succession of zeros in the template. (If f_{c_1} is never iterated, the critical orbit is trivial.) Otherwise, the first nonzero orbit entry will be $\xi_M = f_{c_1}(0) = c_1$, with $|\xi_M| > 2$. This will be squared repeatedly over the next succession of zero template entries. If all the remaining template entries are zero, the orbit will be, for all $n \geq 0$, $\xi_{M+n} = c_1^{2^n}$, with $|\xi_{M+n}| > 2$. If there is at least one additional nonzero entry in the template, at position $M + K$, then $\xi_{M+K} = c_1^{2^K}$, and $\xi_{M+K+1} = c_1^{2^{K+1}} + c_1$. Notice that $|\xi_{M+K+1}| = |c_1^{2^{K+1}} + c_1| = |c_1|(|c_1|^{2^{K+1}-1} - 1) > |c_1| > 2$. Hence ξ_{M+K+1} satisfies the conditions of Lemma 1.5 and the orbit escapes. In either case, once the orbit escapes the disk of radius $R_e = 2$, it continues to increase to ∞ . \square

Proposition 1.8. *For $(c_0, c_1) \in \mathbb{C}^2$ with $|c_0|, |c_1| \leq 2$, the template orbit $(\xi_n)_n$ of $\xi_0 = 0$ under (c_0, c_1) has escape radius $R_e = 2$.*

Proof. The statement follows directly from Lemma 1.5. \square

Remark 1. Clearly, $R_e = 2$ does not act as an escape radius for any arbitrary template iteration. Here is a simple construction for which $R_e = 2$ fails as escape radius. Fix a value of c_0 outside of the traditional Mandelbrot set. We choose the value of c_1 and the template s as follows. According to Theorem 1.4, the orbit of zero will leave the disk of radius $R_e = 2$ after a certain number N of iterations of f_{c_0} , and never return: $0 \rightarrow z_1 \rightarrow z_2 \rightarrow \dots \rightarrow z_N$, with $|z_n| > 2$, for all $n \geq N$. Consider now a point z' in the filled Julia set of f_{c_0} , and choose $c_1 = z' - z_N^2$. Choose the template s to be such that $s_j = 0$, for all $j \neq N + 1$, and $s_{N+1} = 1$. Then the orbit $o_s(0)$ leaves the escape disk in N iterates (since $|z_N| > 2$), but $z_{N+1} = z_N^2 + c_1 = z'$, and the orbit remains henceforth bounded (all future iterations are under f_{c_0}). Notice that the choice that generates this counterexample is not robust, since the filled Julia set is Fatou dust for a c_0 outside of the Mandelbrot set; hence the choice of z' , and subsequently of c_1 , is made from a set of area zero.

2 Structure of fixed-map Mandelbrot sets

In this section, we will study the structure of fixed-map Mandelbrot sets, for different pairs (c_0, c_1) . Since later in the paper we perform a computer-assisted numerical analysis, we will use truncated

templates in order to illustrate our sets. We therefore find it useful to define finitely iterated versions of our sets (that is, Mandelbrot sets for binary templates of finite length N), and explore the limit behavior as $N \rightarrow \infty$.

Definition 2.1. For any integer $N \geq 1$, we call the N -root of the template $\mathbf{s} = (s_n)_{n \geq 1}$ the finite binary sequence $\langle \mathbf{s} \rangle = s_1 \dots s_N$. We will use the notation $\{0, 1\}^N$ for the set of all N -roots. We say that two templates \mathbf{s} and $\mathbf{s}' \in \{0, 1\}^\infty$ have a common N -root if they agree up to the N th position: $s_j = s'_j$, for $1 \leq j \leq N$.

Note. N need not be maximal in order to define a common N -root; if two templates have a common N -root, they will have a common k -root, for all $1 \leq k \leq N$.

Definition 2.2. We will use the notations $o_{\langle \mathbf{s} \rangle}(\xi_0) = o_{\mathbf{s}}^N(\xi_0)$ for the truncated orbit of a point ξ_0 under the N -root $\langle \mathbf{s} \rangle$. We will also use $o_{\mathbf{s}}^j(\xi_0)$ and $o_{\langle \mathbf{s} \rangle}^j(\xi_0)$ to designate specifically the j -th iterate of ξ_0 under an infinite template \mathbf{s} and respectively under an N -root $\langle \mathbf{s} \rangle$.

Definition 2.3. For a fixed pair $(c_0, c_1) \in \mathbb{C}^2$, we define the N -rooted fixed-map Mandelbrot set as:

$$\mathcal{M}_{c_0, c_1}^N = \{\mathbf{s} \in \{0, 1\}^\infty, \text{ with } |o_{\mathbf{s}}^N(0)| < R_e\}$$

With this definition, together with the definition of the fixed-map Mandelbrot set in Section 1.1, we have the following lemma:

Lemma 2.4. For any (c_0, c_1) that satisfy the escape radius and for any arbitrary integer $N \geq 1$ we have that $\mathcal{M}_{c_0, c_1} \subset \mathcal{M}_{c_0, c_1}^{N+1} \subset \mathcal{M}_{c_0, c_1}^N$.

Proof. Suppose $\langle \mathbf{s} \rangle$ is an N -root such that $|o_{\langle \mathbf{s} \rangle}^N(0)| > R_e$ (that is, the orbit of $\xi_0 = 0$ escapes by the time the iteration reaches the end of the N -root). Then none of the templates $\mathbf{s} \in \{0, 1\}^\infty$ with the common N -root $\langle \mathbf{s} \rangle$ are in \mathcal{M}_{c_0, c_1} . □

To better represent subsets of templates with certain properties, we put an order on $\{0, 1\}^\infty$ by identifying each template with the binary expansion of a real number in the unit interval. More precisely, we consider the map:

$$\begin{aligned} \psi: \{0, 1\}^\infty &\rightarrow [0, 1] \\ \psi(\mathbf{s}) &= \sum_{n=1}^{\infty} s_n 2^{-n} \text{ for all } \mathbf{s} = (s_n)_n \end{aligned}$$

Then we can represent the sets \mathcal{M}_{c_0, c_1} and \mathcal{M}_{c_0, c_1}^N as their images in $[0, 1]$, $\psi(\mathcal{M}_{c_0, c_1})$ and respectively $\psi(\mathcal{M}_{c_0, c_1}^N)$ (see Figure 1).

Remark. Notice that ψ is surjective, but not injective, since any number in $[0, 1]$ has at least one binary expansion, but some numbers do have multiple expansions – a finite one, and an infinite one (e.g., $0.1 = 0.0\bar{1}$).

Theorem 2.5. For every (c_0, c_1) satisfying the escape radius condition, \mathcal{M}_{c_0, c_1}^N is a nested sequence of sets with

$$\bigcap_{N=1}^{\infty} \mathcal{M}_{c_0, c_1}^N = \mathcal{M}_{c_0, c_1}$$

Proof. Recall that $\mathcal{M}_{c_0, c_1} \subset \mathcal{M}_{c_0, c_1}^{N+1} \subset \mathcal{M}_{c_0, c_1}^N$, for all $N \geq 1$. Indeed, if $|o_{\mathbf{s}}^{N+1}(0)| < R_e$ for some template \mathbf{s} then, from the escape radius condition, it follows that $|o_{\mathbf{s}}^N(0)| < R_e$ as well, which implies that \mathcal{M}_{c_0, c_1}^N are nested around \mathcal{M}_{c_0, c_1} . Subsequently, the intersection $\bigcap_{N=1}^{\infty} \mathcal{M}_{c_0, c_1}^N \supset \mathcal{M}_{c_0, c_1}$.

On the other hand, if $|o_{\mathbf{s}}^N(0)| < R_e$ for all $N \geq 1$, then $\mathbf{s} \in \mathcal{M}_{c_0, c_1}$. Hence $\bigcap_{N=1}^{\infty} \mathcal{M}_{c_0, c_1}^N \subset \mathcal{M}_{c_0, c_1}$. In

conclusion: $\bigcap_{N=1}^{\infty} \mathcal{M}_{c_0, c_1}^N = \mathcal{M}_{c_0, c_1}$.

□

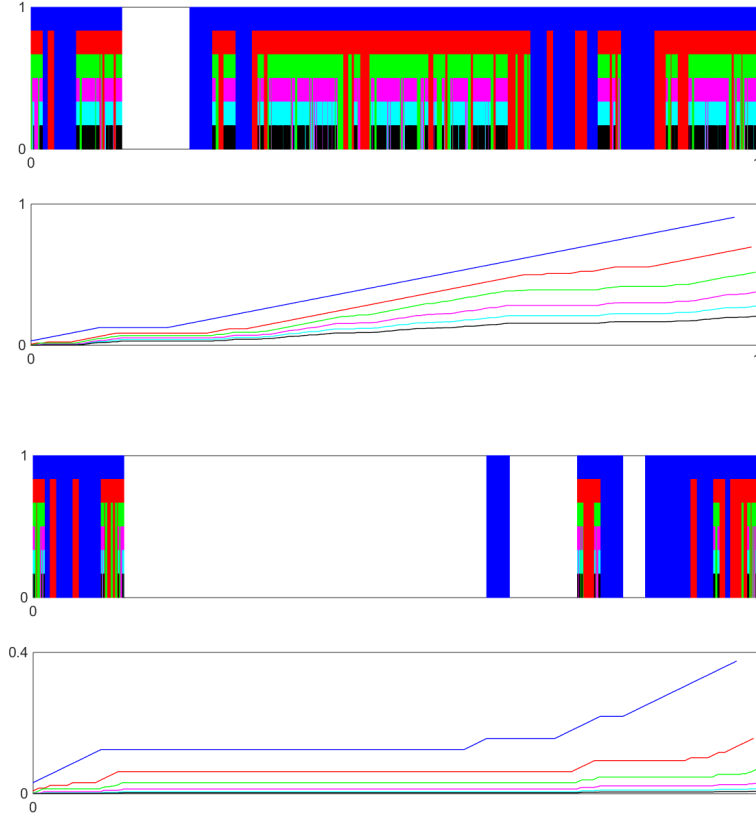


Figure 1: N -rooted fixed-map Mandelbrot sets for two different map pairs (c_0, c_1) : $c_0 = -0.117 - 0.76i$ and $c_1 = -0.62 - 0.62i$ (**top**); $c_0 = -0.75$ and $c_1 = -0.117 - 0.856i$ (**bottom**). The top subplot of each panel shows sets $\psi(\mathcal{M}_{c_0, c_1}^N)$ for different values of N , in different colors: $N = 5$ (blue), $N = 7$ (red), $N = 9$ (green), $N = 11$ (pink), $N = 13$ (cyan), $N = 15$ (black). To make it easier to simultaneously visualize these sets within the same copy of the unit interval, the sets were represented as blocks with height decreasing from 1 to 1/3 for increasing N , layering out their structure for comparison (they are nested sets). The bottom subplot represents the accumulation map for each of the sets on top, in corresponding colors.

Remark. Notice first that the intersection \mathcal{M}_{c_0, c_1} is nonempty if either c_0 or c_1 are in the traditional Mandelbrot set, (\mathcal{M}_{c_0, c_1} contains the all zero template if c_0 is in \mathcal{M} , and it contains the all one template if c_1 is in \mathcal{M}). \mathcal{M}_{c_0, c_1} is empty if both $|c_0| > 2$ and $|c_1| > 2$. The “size” of \mathcal{M}_{c_0, c_1} for intermediate values of c_0 and c_1 will be further discussed in Section 3.

While the proof of Theorem 2.5 is straightforward, we would like to illustrate it for the images of our sets in the unit interval, as we compare $\psi(\mathcal{M}_{c_0, c_1}^N)$ and $\psi(\mathcal{M}_{c_0, c_1})$ in Figure 1. For a fixed N , there are 2^N possible N -roots $\langle \mathbf{s}^0 \rangle = 0 \dots 00$, $\langle \mathbf{s}^1 \rangle = 0 \dots 01$, up to $\langle \mathbf{s}^{2^N} \rangle = 1 \dots 11$, whose images under ψ , together with the endpoint 1, form a partition $(a_j^N)_{1 \leq j \leq 2^N+1}$ of $[0, 1]$: $a_j^N = \psi(\mathbf{s}^j)$, for $j = 0, 2^N$, and $a_{2^N+1}^N = 1$. It is easy to see that $\psi(\mathcal{M}_{c_0, c_1}^N)$ is a union of intervals $[a_j^N, a_{j+1}^N]$. Similarly, $\psi(\mathcal{M}_{c_0, c_1}^{N+1})$ is a union of intervals $[a_j^{N+1}, a_{j+1}^{N+1}]$ formed by points in the partition generated by all $(N+1)$ -roots. Note that (a_j^{N+1}) is a finer partition than (a_j^N) , since it contains all points in (a_j^N) and the midpoints between those. Suppose now that an interval $[a_j^{N+1}, a_{j+1}^{N+1}] \subset \psi(\mathcal{M}_{c_0, c_1}^{N+1})$. This means that the last iterate of zero under the $(N+1)$ -root $\langle \mathbf{s} \rangle = \psi^{-1}(a_j^{N+1})$ is inside the escape disc. Subsequently, all the previous iterates under $\langle \mathbf{s} \rangle = s_1 s_2 \dots s_{N+1}$ have to also be inside the escape disc. Consider the N th root $\langle \mathbf{s}' \rangle = s_1 s_2 \dots s_N$, and take $a_i^N = \langle \psi(\mathbf{s}') \rangle$. It follows that $[a_j^{N+1}, a_{j+1}^{N+1}] \subset [a_i^N, a_{i+1}^N]$, in other words every interval in $\psi(\mathcal{M}_{c_0, c_1}^{N+1})$ is part of a subinterval in $\psi(\mathcal{M}_{c_0, c_1}^N)$. Figure 1 represents the sets $\psi(\mathcal{M}_{c_0, c_1}^N)$ in different colors for different values of N . In order to make the nested property more visible, we plotted them as 2-dimensional “combs” $\psi(\mathcal{M}_{c_0, c_1}^N) \times [0, h]$, where the height h decreases with the value of N (so that one can observe the layering of nested combs of different colors as N increases).

We define the *accumulation map* for each \mathcal{M}_{c_0, c_1}^N as follows. Consider $\{0, 1\}^N = \{\langle \mathbf{s}^1 \rangle, \dots, \langle \mathbf{s}^{2^N} \rangle\}$ the set of all N -roots, and their corresponding partition $(a_j^N)_{1 \leq j \leq 2^N+1}$, as defined above. Then the accumulation map is given by:

$$\phi_{c_0, c_1}^N : [0, 1] \rightarrow [0, 1]$$

$$\phi_{c_0, c_1}^N(t) = \begin{cases} 0, & \text{at } t = 0 \\ \phi(a_j^N) & \text{on } [a_j^N, a_{j+1}^N], \text{ if } \langle \mathbf{s}^j \rangle \notin \mathcal{M}_{c_0, c_1}^N \\ \phi(a_j^N) + t - a_j^N & \text{on } [a_j^N, a_{j+1}^N], \text{ if } \langle \mathbf{s}^j \rangle \in \mathcal{M}_{c_0, c_1}^N \end{cases}$$

In other words, the map starts at $\phi(0) = 0$, increases by $1/2^N$ on each subinterval which of $\psi(\mathcal{M}_{c_0, c_1}^N)$, and remains constant on each interval which is not in $\psi(\mathcal{M}_{c_0, c_1}^N)$. Since the sets $\psi(\mathcal{M}_{c_0, c_1}^N)$ are nested, and the corresponding partition (a_j^N) becomes finer with increasing N , it follows that the accumulation map becomes lower as N increases. The bottom subplots in Figure 1 show, in two separate panels for two different fixed pairs (c_0, c_1) , a few instances of ϕ_{c_0, c_1}^N , for the same values of N for which the corresponding $\psi(\mathcal{M}_{c_0, c_1}^N)$ sets are plotted in the top subplots.

Consider now the point-wise limit of $\phi_{c_0, c_1} = \lim_{N \rightarrow \infty} \phi_{c_0, c_1}^N$. This is also a positive, monotonely increasing map of the interval, which we will call the *accumulation map* of \mathcal{M}_{c_0, c_1} . Some of the topological structure of \mathcal{M}_{c_0, c_1} for different pairs (c_0, c_1) can be captured by looking at the structure of the corresponding accumulation map ϕ_{c_0, c_1} , with patterns reminiscent of a devil’s staircase.

The structure of the graph of the accumulation map is specific to the order put on templates (via the map ψ). For our particular order on $\{0, 1\}^\infty$, its maximum value occurs at the end, for $t = 1$. We will call this value the *full template value* of the pair (c_0, c_1) , the limit of the *full N -root values* of (c_0, c_1) : $\phi_{c_0, c_1}(1) = \lim_{N \rightarrow \infty} \phi_{c_0, c_1}^N(1)$. The value can be interpreted as the likelihood for a random template in $\{0, 1\}^\infty$ to deliver a bounded critical orbit $o_{\mathbf{s}}(0)$ under the iterations of f_{c_0} and f_{c_1} specified by the template \mathbf{s} .

Definition 2.6. *We will say that the pair (c_0, c_1) is N -well behaved if the corresponding full N -root value $\phi_{c_0, c_1}^N(1) = 1$. We will say that the pair is infinitely well behaved if the full template value $\phi_{c_0, c_1}(1) = 1$.*

Remark. In other words, a pair (c_0, c_1) is N -well behaved if the first N iterates of the critical point remain inside the escape disc for *all* N -roots, for the given functions f_{c_0} and f_{c_1} . A pair is infinitely well behaved if it is N -well behaved for all N . This is equivalent to requesting that the critical orbit remain bounded under iterations of fixed f_{c_0} and f_{c_1} , for almost all templates (seen as numbers on the unit interval, with the Lebesgue probability measure).

One potential direction to pursue would be to analyze the topological structure of the graph of the accumulation map. In particular, we can investigate the frequency of plateaus of different lengths; for “devil’s staircase” type graphs, this dependence follows a power law. In Figure 2, we represent this dependence for the same (c_0, c_1) parameter pairs for which the accumulation maps are shown in Figure 1. For fixed $N = 20$, we consider all possible plateau lengths $1 \leq l \leq 2^N$. For each l , we denote by $s(l)$ the number of all plateaux with length l . In the two figure panels, we represent $\log(s+1)$ versus $\log(l)$ (one was added to s in order to avoid getting an undefined value for lengths which are not represented). While the value of N used for both plots is $N = 20$ (making it too small to extrapolate the behavior as $N \rightarrow \infty$), the plots are reminiscent of log-log linear behavior. In future work, we can explore computationally the structure of these plots for higher values of N , as well as for a more complex version of the accumulation map, considering orbits of all critical points (that appear at all steps in the iteration sequence).

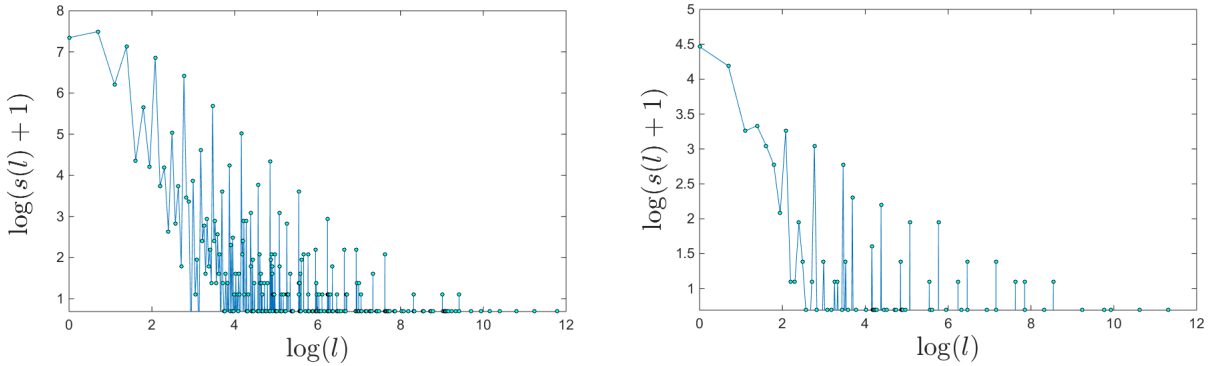


Figure 2: **Log-log representation of the distribution of plateau lengths** for $N = 20$ and parameters $c_0 = -0.117 - 0.76i$ and $c_1 = -0.62 - 0.62i$ (left); $c_0 = -0.75$ and $c_1 = -0.117 - 0.856i$ (right).

A related direction of potential interest is to study the topological structure of the fixed-map Mandelbrot set $\psi(\mathcal{M}_{c_0, c_1})$, as the parameters c_0 and c_1 are begin varied. In the following section, we examine an easier dependence: that of the value $\phi_{c_0, c_1}(1)$ on the complex parameter pair (c_0, c_1) .

3 Hybrid, contour and multi-Mandelbrot sets

Fix now $c_0 \in \mathbb{C}$. With the notation from Section 2, the *hybrid Mandelbrot set* corresponding to c_0 is:

$$\mathcal{M}_{c_0} = \{(c_1, b) \in \mathbb{D}(R_e) \times [0, 1], \text{ with } b = \phi_{c_0, c_1}(1)\}$$

where $\mathbb{D}(R_e)$ is the complex disc of radius $R_e = \max\{2, |c_0|, |c_1|\}$. As before, one can also define *root hybrid* sets:

$$\mathcal{M}_{c_0}^N = \{(c_1, b) \in \mathbb{D}(R_e) \times [0, 1], \text{ with } b = \phi_{c_0, c_1}^N(1)\}$$

Figure 3a illustrates the root hybrid set for $c_0 = 0$, for a root length of $N = 20$, with the value b corresponding to each c_1 represented as a color from blue to dark red. For $c_0 = 0$, the critical orbit will always be bounded when using the template with all entries zero. With the color map in

Figure 3a, the blue region represents the values of c_1 for which $\langle s \rangle = 0 \dots 0$ is the only N -root that confines the critical orbit to the escape disc. The dark red central region represents the values of c_1 for which *all* N -roots confine the critical orbit to the escape disc $\mathbb{D}(R_e)$. In other words, this is the region of c_1 for which the pair $(0, c_1)$ is N -well behaved.

Figure 3b illustrates the central plateau of the hybrid set by comparison with an approximation of the traditional Mandelbrot set \mathcal{M} , computed based on the same number N of iterates. The former is a subset of the latter, property which remains true in the limit of $N \rightarrow \infty$:

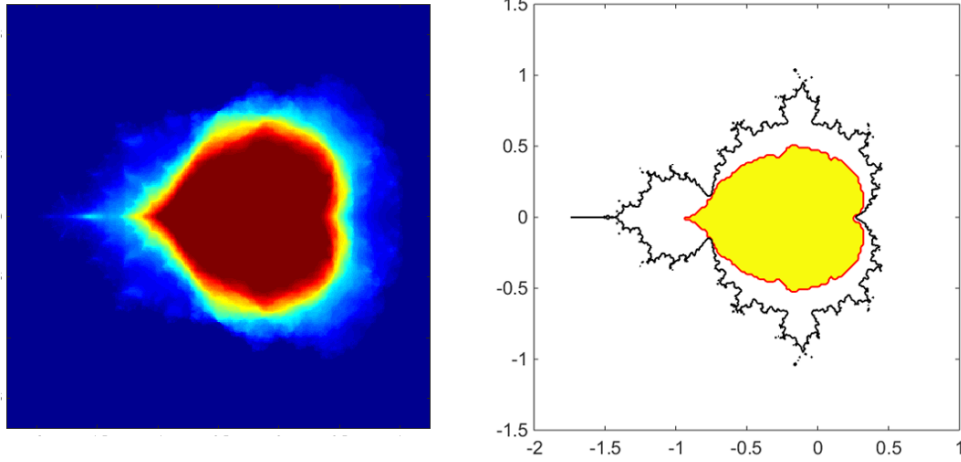


Figure 3: **Root hybrid Mandelbrot set \mathcal{M}_0^N for $N = 20$.** **Left.** Each pair (c_1, b) is represented as a point c_1 in the complex plane with an associated color from blue to dark red for $b = \phi_{0, c_1}^N(1)$ increasing from 0 to 1. **Right.** The shaded region corresponds to the N -well behaved pairs $\phi_{0, c_1}^N(1) = 1$ for $N = 20$. It is illustrated as a subset of a truncated representation of the traditional Mandelbrot set, based for comparison on $N = 20$ iterations as well (the interior of the black curve).

$$\{c_1 \in \mathbb{D}(2) \text{ with } \phi_{0, c_1}(1) = 1\} \subset \mathcal{M} \subset \mathbb{D}(2)$$

Theorem 3.1. *The set of infinitely well-behaved pairs $(0, c_1)$ contains the disc centered at the origin, of radius $1/4$.*

Proof. Consider $c_1 \in \mathbb{C}$, with $|c_1| < 1/4$. Then $\Delta = 1 - 4|c_1| > 0$, and one can define $d = \frac{1 + \sqrt{\Delta}}{2} = \frac{1 + \sqrt{1 - 4|c_1|}}{2}$. Notice that $0 < d < 1$. Suppose now that $|z| < d$. It follows that

$$|z^2 + c_1| \leq |z|^2 + |c_1| \leq d^2 + |c_1| = \frac{1 + 2\sqrt{\Delta} + \Delta}{4} + |c_1| = \frac{1 + \sqrt{\Delta}}{2} = d$$

Subsequently, if $|z| < d$ then $|f_{c_{s_n}}(z)| < d$, for all $n \geq 1$. Inductively, it follows that the orbit of $\xi_0 = 0 < d$ is completely contained in the disc of radius d around the origin, hence it is bounded. In conclusion: the critical orbit is bounded for all possible template iterations under the pair of maps $(0, c_1)$ with $|c_1| < 1/4$. In other words, the parameter disc centered at the origin and of radius $1/4$ is a subset of the set of infinitely well-behaved pairs $(0, c_1)$. \square

Based on our simulations, we conjecture the following:

Conjecture 3.2. *The set of infinitely well-behaved pairs $(0, c_1)$ is star-shaped connected.*

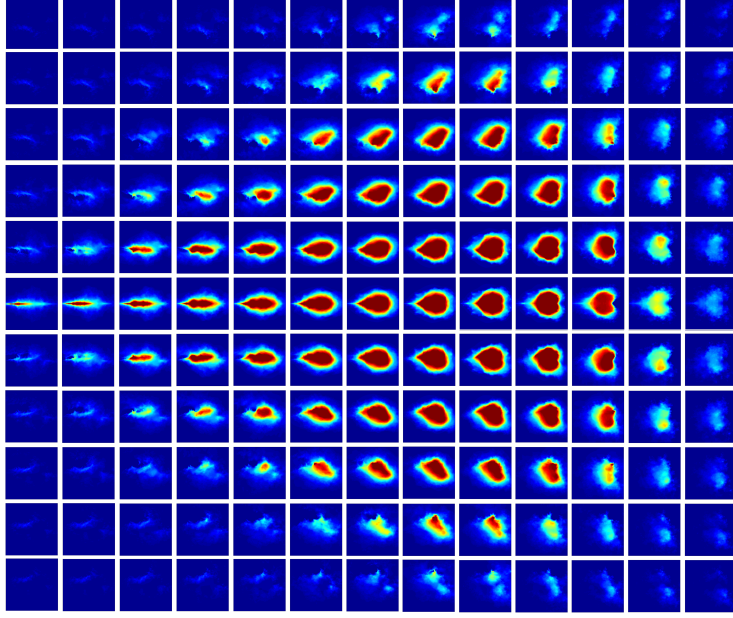


Figure 4: **Hybrid sets for a grid of c_0 values.** Each panel represents one value of c_0 , covering the interval $[-1.6, 0.8]$ along the real axis and $[-1, 1]$ along the imaginary axis, with distance 0.2 in between sample values in both directions.

While the hybrid set for $c_0 = 0$ may be the easiest to study and understand, one can consider hybrid sets for other values of c_0 . Figure 4 illustrates the hybrid sets for a grid of c_0 complex values with $\text{Re}(c_0) \in [-1.6, 0.8]$, and $\text{Im}(c_0) \in [-1, 1]$. There are a few different ways in which one can organize this atlas of c_0 -indexed hybrid sets. Below we describe two such ways, by defining two new sets:

Definition 3.3. *The contour Mandelbrot set is defined as*

$$\mathcal{CM} = \{(c_0, b) \in \mathbb{D}(2) \times [0, 1], \text{ with } b = \max(\Pi_2(\mathcal{M}_{c_0}))\}$$

where $\Pi_2(\mathcal{M}_{c_0})$ designates the second component of the hybrid set \mathcal{M}_{c_0} . Similarly, one can define the N -root contour Mandelbrot set as

$$\mathcal{CM}^N = \{(c_0, b) \in \mathbb{D}(2) \times [0, 1], \text{ with } b = \max(\Pi_2(\mathcal{M}_{c_0}^N))\}$$

The contour Mandelbrot set assigns to every $c_0 \in \mathbb{D}(2)$ the largest value of $\phi_{c_0, c_1}(1)$ over all $c_1 \in \mathbb{D}(2)$. Similarly, one can assign to every c_0 the largest value of $\phi_{c_0, c_1}^N(1)$, and obtain the N -root mega-hybrid set – illustrated in Figure 5a for $N = 8$, with the colors representing, as before, different values of b .

One can consider the central (burgundy) plateau of \mathcal{CM}^N , representing all the values of $c_0 \in \mathbb{D}(2)$ for which there exists a $c_1 \in \mathbb{D}(2)$ such that (c_0, c_1) is N -well behaved. In Figure 5b, we illustrate the fact that the N -truncated Mandelbrot set is a subset of this central plateau, for all N . In the $N \rightarrow \infty$ limit, the Mandelbrot set is included in the set of $c_0 \in \mathbb{D}(2)$ for which there is at least one c_1 with (c_0, c_1) infinitely well behaved.

Definition 3.4. *The multi-Mandelbrot set is defined as*

$$\mathcal{MM} = \{(c_0, c_1) \in \mathbb{D}^2(2), \text{ such that } \phi_{c_0, c_1}(1) = 1\}$$

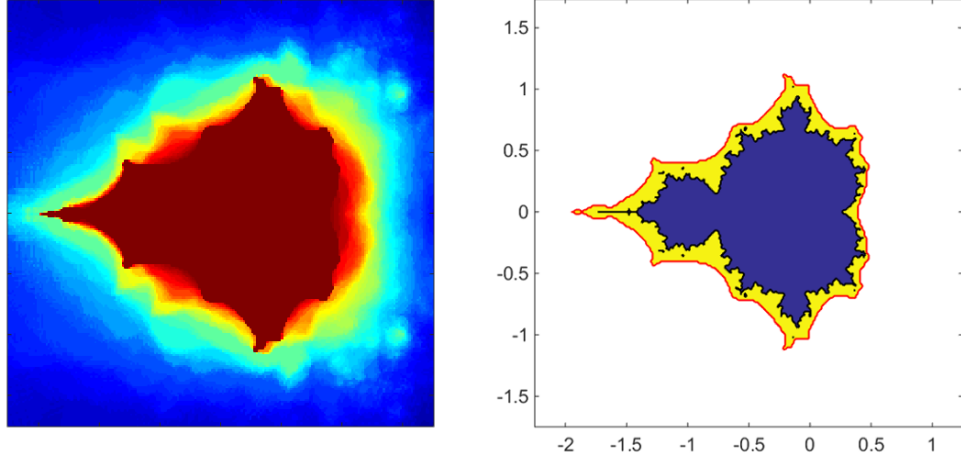


Figure 5: ***N -root contour Mandelbrot set**, for $N = 8$. **Left.** The colors represent values of b from zero (blue) to 1 (dark red). **Right.** The yellow region represents the central plateau of \mathcal{CM}^N for $N = 20$. In blue is shown an approximation of the classical Mandelbrot set \mathcal{M} , for the same $N = 20$.*

and the N -root super-hybrid Mandelbort set is

$$\mathcal{MM}^N = \{(c_0, c_1) \in \mathbb{D}^2(2), \text{ such that } \phi_{c_0, c_1}^N(1) = 1\}$$

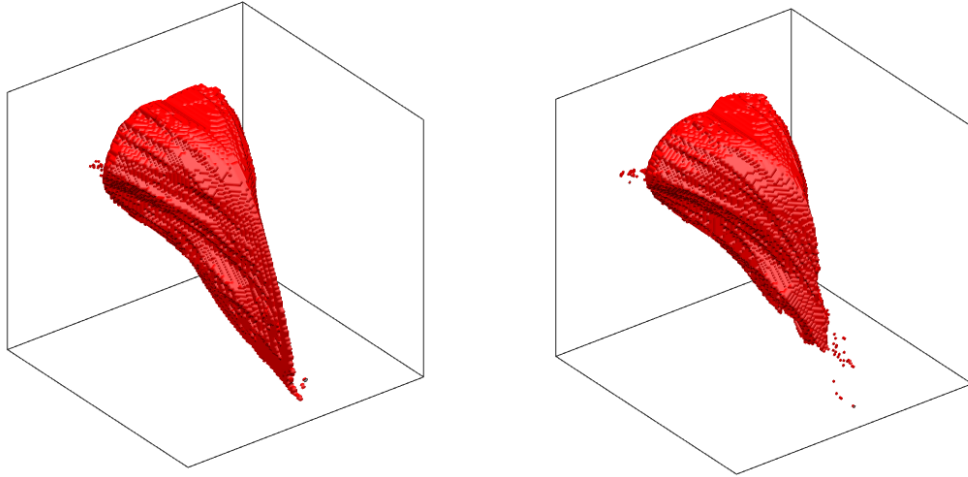


Figure 6: **Three-dimensional slices of the N -root multi-Mandelbrot set**, for $N=8$. **Left.** Real $c_0 \in [-2, 1]$. **Right.** Complex $c_0 = \text{Re}(c_0) + 0.1i$, with $\text{Re}(c_0) \in [-2, 1]$.

\mathcal{MM} is the set of all infinitely well behaved parameter pairs in $\mathbb{D}(2) \times \mathbb{D}(2)$. Both \mathcal{MM} and \mathcal{MM}^N have complex dimension 2 (or real dimension 4). In Figure 6, we illustrate 3-dimensional slices of \mathcal{MM}^N . While Figure 6 shows that not all 3D slices of \mathcal{MM}^N are connected, we conjecture that:

Conjecture 3.5. *\mathcal{MM} is a connected set in \mathbb{C}^4 .*

4 Multicritical definitions

Our condition for the critical point at zero to have a bounded orbit, while inspired by its relevance to potential applications, differs from the postcritically bounded condition typically used in the context of random iterations [8]. In order to reconcile our results with this framework, we investigate whether the same objects can be studied when using the alternate definition, in which *all* critical points, generated at all stages of the iteration, are required to remain bounded (we will call the corresponding sets **multi-critical M-sets**).

This idea follows naturally when one thinks of what the definition of a critical point should be for a non-autonomous iteration. Suppose one iterates consecutively k differentiable functions f_1 to f_k , having a critical point for the composition requires (using the Chain Rule multiple times) that:

$$(f_k \circ f_{k-1} \circ \dots \circ f_2 \circ f_1)'(z) = f_k'[f_{k-1} \circ \dots \circ f_2 \circ f_1(z)] \cdot \dots \cdot f_2'[f_1(z)] \cdot f_1'(z) = 0$$

Hence z is a critical point for the composition if either z is a critical point for f_1 , or $f_{k-1} \circ \dots \circ f_2 \circ f_1(z)$ is a critical point for f_k , for some $k \geq 1$. In the case of template iterations, we are applying a sequence of quadratic functions $f_{c_0}(z)$ and $f_{c_1}(z)$. The situation is quite simple, because, at each step, the function we are iterating has only one critical point $\xi_0 = 0$ (independently on the step). So an efficient computational strategy for determining whether a polynomial sequence is postcritically bounded consists of checking whether the tails or the orbits below are bounded or whether they escape to ∞ :

$$\begin{array}{ccccccc} 0 & \xrightarrow{f_{c_{s_1}}} & * & \xrightarrow{f_{c_{s_2}}} & * & \xrightarrow{f_{c_{s_3}}} & * & \xrightarrow{f_{c_{s_4}}} & * & \dots & \xrightarrow{f_{c_{s_k}}} & * & \xrightarrow{f_{c_{s_{k+1}}}} & \dots \\ & & 0 & \xrightarrow{f_{c_{s_2}}} & * & \xrightarrow{f_{c_{s_3}}} & * & \xrightarrow{f_{c_{s_4}}} & * & \dots & \xrightarrow{f_{c_{s_k}}} & * & \xrightarrow{f_{c_{s_{k+1}}}} & \dots \\ & & & & 0 & \xrightarrow{f_{c_{s_3}}} & * & \xrightarrow{f_{c_{s_4}}} & * & \dots & \xrightarrow{f_{c_{s_k}}} & * & \xrightarrow{f_{c_{s_{k+1}}}} & \dots \\ & & & & & & \vdots & & & & & & & \\ & & & & & & 0 & \xrightarrow{f_{c_{s_4}}} & * & \dots & \xrightarrow{f_{c_{s_k}}} & * & \xrightarrow{f_{c_{s_{k+1}}}} & \dots \\ & & & & & & & & 0 & \xrightarrow{f_{c_{s_k}}} & * & \xrightarrow{f_{c_{s_{k+1}}}} & \dots \end{array}$$

Hence we consider the following alternative definitions, which consider all critical points generated throughout the iteration:

Definition 4.1. Fix $\mathbf{s} \in \{0, 1\}^\infty$ a symbolic sequence. The corresponding **multi-critical fixed-template Mandelbrot set** is defined as:

$${}^m\mathcal{M}_{\mathbf{s}} = \{(c_0, c_1) \in \mathbb{C}^2, \text{ where } o_{\mathbf{s}^k}(0) \text{ is bounded for all integers } k \geq 0\}$$

where \mathbf{s}^k is the right k -shift of the template \mathbf{s} .

Definition 4.2. Fix $(c_0, c_1) \in \mathbb{C}^2$. The corresponding **multi-critical fixed-map Mandelbrot set** is defined as:

$${}^m\mathcal{M}_{c_0, c_1} = \{\mathbf{s} \in \{0, 1\}^\infty, \text{ where } o_{\mathbf{s}^k}(0) \text{ is bounded for all integers } k \geq 0\}$$

Definition 4.3. For a fixed $c_0 \in \mathbb{C}$, the **multi-critical hybrid Mandelbrot set** is defined as:

$${}^m\mathcal{M}_{c_0} = \{(c_1, b) \in \mathbb{C} \times [0, 1], \text{ with } b = \mathcal{L}({}^m\mathcal{M}_{c_0, c_1})\}$$

where \mathcal{L} designates the Lebesgue measure on the interval $[0, 1]$.

Figure 7 shows a few examples of multi-critical M-slices for fixed $c_0 = 0$ and for fixed templates with specific frequencies of iterating one function versus the other. These sets are presented in comparison with their regular M-slice counterparts, of which they are subsets.

As in the previous section, we obtain a more comprehensive view by computing multi-critical *hybrid* sets. For illustration purposes, we consider the same parameter values $c_1 \in \mathbb{C}$ as in Figure 4 in Section 3, and show in Figure 10, side by side, the tables for regular hybrid slices and for multi-critical hybrid slices. Notice that the burgundy plateaux are identical between the two figures, for all c_0 panels (as justified in the following section). Moreover, the regular and multi-critical hybrid sets differ less when c_0 is close to the origin, and more in the panels for c_0 away from the origin.

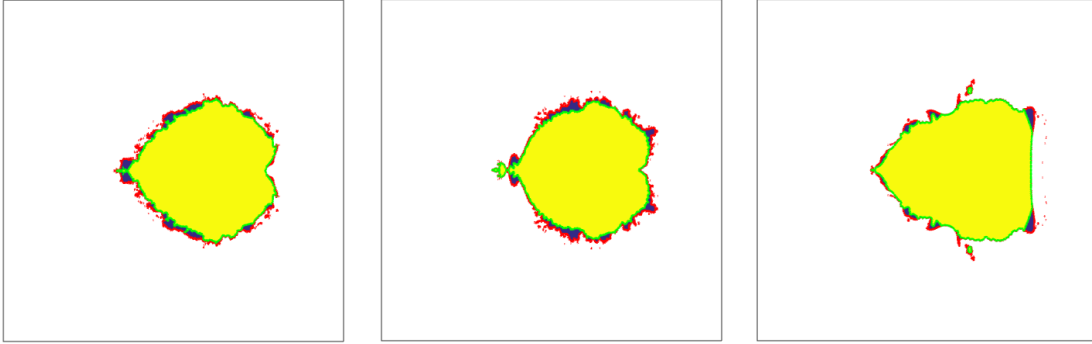


Figure 7: **Examples of fixed-template M-slices and multi-critical M-slices for $c_0 = 0$.** The template \mathbf{s} was selected at random such that **A.** the probability of a 1 entry is $p = 0.5$; **B.** the probability of a 1 entry is $p = 0.25$; **C.** the probability of a 1 entry is $p = 0.75$. The larger region (red contour, shaded in blue) represents the M-slice for $c_0 = 0$, which is the subset $c_1 \in \mathbb{C}$ for which the original critical point $\xi_0 = 0$ is bounded under the maps (c_0, c_1) with template \mathbf{s} . The nested region (green contour, shaded yellow) represents the multi-critical M-slice, which is the subset of $c_1 \in \mathbb{C}$ for which the whole critical set (consisting of $\xi_0 = 0$ from all iteration steps, as described in the text) is bounded under the iteration system.

4.1 Fatou-Julia theorem

A great rationale for using the multi-critical definition for the Mandelbrot sets is the relationship of this condition with the topology of the template Julia set. A ubiquitous phenomenon in both real and complex dynamics is that the behavior of a map's critical set encompasses the whole dynamic behavior of the map. Within the complex quadratic family $f_c(z) = z^2 + c$ (with a unique critical point at $z_0 = 0$ for all maps), it is well-known that a bounded orbit for $z_0 = 0$ (i.e., c in the Mandelbrot set) is equivalent to connectedness of the Julia set $J(f_c)$, and that an escaping orbit for $z_0 = 0$ is equivalent to the Julia set being totally disconnected. This duality stands more generally for polynomials P of degree $d \geq 2$, where the Julia set $J(P)$ is connected (a cellular set, in fact) iff it contains all finite critical points of P , and it has uncountably many connected components iff at least one of the critical points escapes (see, for example Theorem 17.3 in [14], or Theorem 3.1 in [5]).

We want to check if this duality still holds in the context of template iterations. Clearly, the result follows trivially in the case of periodic templates, since the system is equivalent in this case with the iteration of a single polynomial of higher degree, with critical orbits identical with those initiated at all steps of the template iteration. We illustrate this in Figure 8, for the periodic template $\mathbf{s} = [011]$, showing that the multi-critical Mandelbrot set coincides in this case with the connectedness locus of the Julia set in \mathbb{C} .

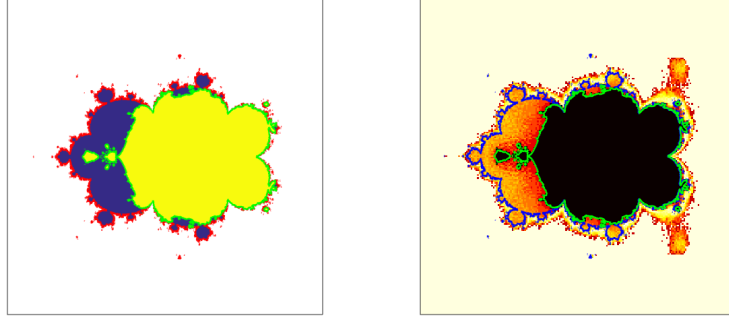


Figure 8: **Mandelbrot slice, multicritical Mandelbrot slice and connectedness slice for fixed periodic template $s = [011]$ and fixed $c_0 = 0$.** **A.** The Mandelbrot slice is the blue interior of the red curve. The multicritical Mandelbrot slice is the yellow interior of the green curve, which is a subset of the former. **B.** The panel illustrates the connectedness locus of the Julia set in the slice $c_0 = 0$, with colors in the hot (red to yellow) spectrum representing the number of connected components of the Julia set, estimated numerically. Black represents the parameters c_1 for which the template Julia set has a single connected component (the connectedness locus), and the outside (white) region represents the locus where the Julia set is totally disconnected. The intermediate lighter to darker colors represent Julia sets with increasingly more connected components. The boundary of the corresponding Mandelbrot and multicritical Mandelbrot slices (shown in **A**) are overlaid as blue and respectively green curves, for comparison.

For random iterations, the traditional dichotomy of the Julia sets having either one or infinitely many connected components clearly fails, and one can easily find examples of Julia sets with a finite number ≥ 2 of connected components. We want to investigate, however, whether the equivalence between the postcritically bounded locus and the Julia set connectedness locus remains valid for templates which are not periodic. This problem has been extensively discussed by Hiroki Sumi, in the wider context of polynomial semigroups. In general, the answer is *no*, and a counterexample is presented as Example 1.7 in [15]. However, the same reference provides a set of sufficient conditions for a postcritically bounded polynomial semigroup to have a connected Julia set (Theorem 2.14 in [15]):

Theorem [15]. Consider a finitely generated polynomial semigroup $G = \langle h_1, \dots, h_n \rangle$ such that each polynomial in G has degree at least 2 and whose finite postcritical set is bounded in \mathbb{C} . Let $a(h)$ be the leading coefficient of each $h \in G$, and in particular call $a_j = a(h_j)$ for all generators $1 \leq j \leq n$. For every $h \in G$, define $\psi(h)(x) = \deg(h)x + \log|a(h)|$, for all $x \in \mathbb{R}$. Let $\alpha = \min \left\{ \frac{\log|a_j|}{1 - \deg(h_j)}, 1 \leq j \leq n \right\}$, and $\beta = \max \left\{ \frac{\log|a_j|}{1 - \deg(h_j)}, 1 \leq j \leq n \right\}$. If $[\alpha, \beta] \subset \bigcup_{j=1}^n \psi(h_j)^{-1}([\alpha, \beta])$, then the Julia set $J(G)$ is connected.

In our case, since $G = \langle h_1, h_2 \rangle$, with $h_1(z) = z^2 + c_0$ and $h_2(z) = z^2 + c_1$, we have $a_j = 1$ and $\deg(h_j) = 2$, for $j = 1, 2$. Hence $\alpha = \beta = 0$, and $\psi(h_1)(x) = \psi(h_2)(x) = 2x$, for all $x \in \mathbb{R}$. It follows that $\psi(h_1)^{-1}(0) = \psi(h_2)^{-1}(0) = 0$, so that $\bigcup_{j=1,2} \psi(h_j)^{-1}([\alpha, \beta]) = \{0\} = [\alpha, \beta]$, and

the condition for the theorem is satisfied. Hence the Julia set connectedness locus and the multicritical Mandelbrot set are identical in this case as well. In Figure 9, we support this result with an illustration based on increasingly tighter computational estimates of these sets, obtained for 50 and respectively 200 iterates along a random template. While the result does not come across when only

using the $N = 50$ root, the boundary of the connectedness locus appears to be trapped between the boundary of the regular Mandelbrot slice and that of the multi-critical Mandelbrot slice, with these outer two boundaries approaching in the limit of N , and squeezing the connectedness boundary in between. This possibly general result for random templates, only suggested here by the numerical simulation, is subject to our current work on the topology of individual Mandelbrot slices.

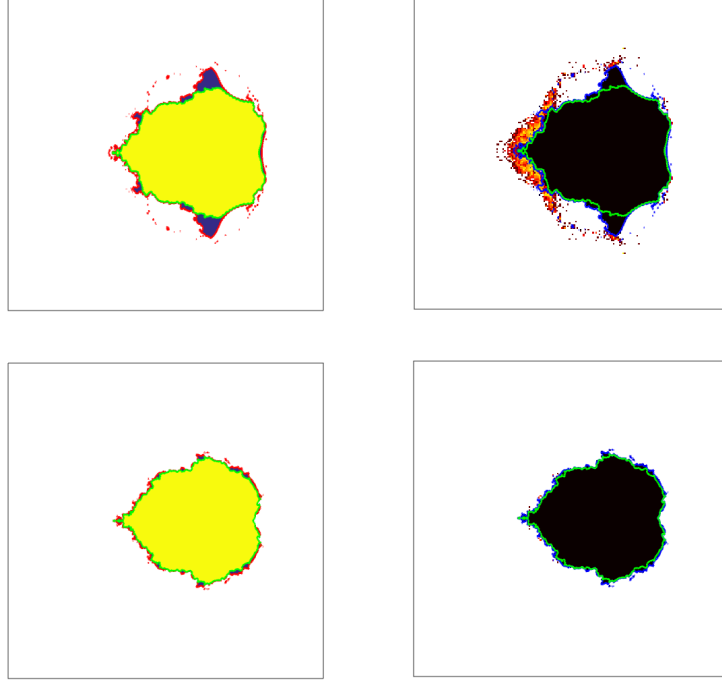


Figure 9: **Mandelbrot slice, multicritical Mandelbrot slice and connectedness slice for $c_0 = 0$ and a random template.** The top panels illustrate these objects using a an approximation based on a 50 entry root of the template; the bottom panels show a refinement, based on a longer root of 200 entries of the same template. **Left.** In each case, the Mandelbrot slice is the blue interior of the red curve. The multicritical Mandelbrot slice is the yellow interior of the green curve, which is a subset of the former. **Right.** The panels illustrate the connectedness of the Julia set in the slice $c_0 = 0$, with colors in the hot (red to yellow) spectrum representing the number of connected components of the Julia set, estimated numerically. Black represents the parameters one connected component (the connectedness locus), and the outside (white) region represents the locus where the Julia set is totally disconnected. The intermediate lighter to darker colors represent Julia sets with increasingly more connected components. The boundary of the corresponding Mandelbrot and muticritical Mandelbrot slices (shown on the left) are overlaid as blue and respectively green curves, for comparison.

4.2 Hybrid sets

Section 4.1 shows that, at the level of each specific template iteration (for fixed parameters c_0 and c_1 , and a fixed template s), the multi-critical Mandelbrot set contains more relevant information about the system than the regular Mandelbrot set. However, for practical purposes, a regular Mandelbrot set is computationally less expensive. In mind with the goal of investigating “averaged” information over all templates (useful for applications), we want to investigate whether one definition remains superior to the other in the context of hybrid Mandelbrot sets.

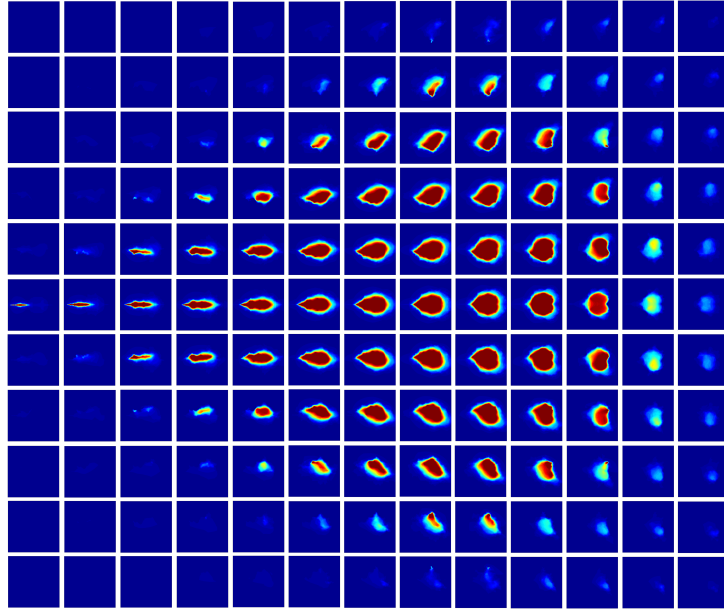


Figure 10: **Multicritical hybrid sets for a grid of c_0 values.** The grid covers $[-1.6, 0.8]$ along the real axis and $[-1, 1]$ along the imaginary axis, with distance 0.2 in between sample values in both directions. All panels are based on N -root approximations with $N = 8$ iterations.

Definition 4.4. We define the multi-critical contour Mandelbrot set as

$${}^m\mathcal{CM} = \{(c_0, b) \in \mathbb{D}(2) \times [0, 1], \text{ with } b = \max(\Pi_2({}^m\mathcal{M}_{c_0}))\}$$

where $\Pi_2({}^m\mathcal{M}_{c_0})$ designates the second component of the multi-critical hybrid set ${}^m\mathcal{M}_{c_0}$.

Definition 4.5. We define the multi-critical multi-Mandelbrot set as

$${}^m\mathcal{MM} = \{(c_0, c_1) \in \mathbb{D}^2(2), \text{ such that the iteration is postcritically bounded for almost all templates}\}$$

Proposition 4.6. Both the multi-Mandelbrot sets and the central plateaux of the contour-Mandelbrot sets are identical with between the two definitions.

Proof. If the original critical point $\xi_0 = 0$ is bounded under any possible template N -root $\langle \mathbf{s} \rangle$ of a fixed pair of maps (c_0, c_1) , then the other fixed points are also bounded, since their iterated orbits are only permutations of the original one. This remains true as $N \rightarrow \infty$. While the contour Mandelbrot sets differ by the two definitions, their central plateaux are identical (see Figure 11), and so are the multi-Mandelbrot sets. \square

It is useful that the two definitions are interchangeable at the level of these averaged sets. One of the advantages is the possibility to compute these sets using the more efficient definition (with one critical point), yet obtain the connectedness of the Julia set delivered by the stricter (multi-critical) definition, as discussed in Section 4.1. In Section 5, we further discuss the relationships between the two means of computing these sets, and we interpret this in the context of applications.

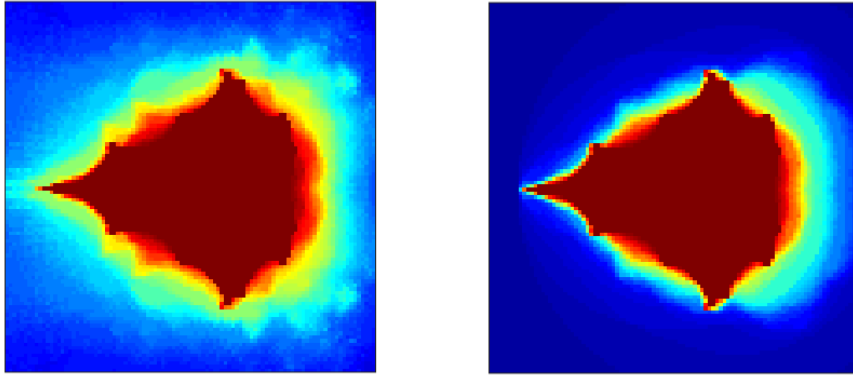


Figure 11: **Contour Mandelbrot sets** for the regular (left) and multi-critical (right) definitions. For each point $c_0 \in \mathbb{C}$, the color represents the value of the maximum likelihood b , in the space of templates of length $N = 8$, for the critical orbit(s) to be bounded, with the maximum taken over all $c_1 \in \mathbb{C}$. The color map ranges from zero (blue) to 1 (dark red).

5 Discussion

5.1 Interpretation of our results

In this paper, we expanded our study of asymptotic dynamics under template iterations, introducing new concepts and ideas for further research. Inspired by one of the alternative definitions of the traditional Mandelbrot set for single map iterations, we investigated extensions in the new context of template iterations. Since in this case the parameters are a combination of the complex value pair $(c_0, c_1) \in \mathbb{C}^2$ and the template $\mathbf{s} \in \{0, 1\}^\infty$, we defined a few different types of parameter slices, which can be more easily visualized and understood than the whole set in $\mathbb{C}^2 \times \{0, 1\}^\infty$.

We first embraced an application-driven idea, and viewed the Mandelbrot set as the parameter locus for which the initial resting state (i.e. the initial condition $\xi_0 = 0$, also the critical point of all maps in the quadratic family) remains bounded under iterations. For fixed (c_0, c_1) , the fixed-map Mandelbrot set designated the set of templates, identified as a subset of the unit interval, for which the critical orbit stays bounded. These sets were found to be unions of subintervals in $[0, 1]$, with structure tightly dependent on the fixed (c_0, c_1) pair. We suggested that the distribution of these subintervals' lengths should be further investigated for power-law behavior. To study the Lebesgue measure of fixed-map Mandelbrot sets in $[0, 1]$, we proceeded to define and analyze hybrid Mandelbrot sets.

For any fixed $c_0 \in \mathbb{C}$, the hybrid Mandelbrot slice was defined as an object in $\mathbb{C} \times [0, 1]$, which can be visualized as a surface, or color plot: for any c_1 in the complex plane, the height/color is assigned based on the likelihood that a random template will keep the critical orbit bounded when iterated in conjunction with the pair of maps (f_{c_0}, f_{c_1}) . If, as proposed in the Introduction, we think of the fixed f_{c_0} as the “correct” iteration map, the hybrid set \mathcal{M}_{c_0} identifies, for each $c_1 \in \mathbb{C}$, how likely it is for the system initiated from rest to evolve along a sustainable (i.e., bounded) trajectory when randomly interposing “erroneous” maps f_{c_1} in the iteration. In each $\mathbb{C} \times [0, 1]$ hybrid plot, this likelihood can vary theoretically between 0 and 1. However, the maximum of 1 will not be necessarily achieved by all hybrid sets. As illustrated by Figure 4, the peaks of the hybrid sets generally get lower as $|c_0|$ increases, but they do so in a non-trivial way.

To describe this phenomenon, we defined the contour Mandelbrot set, associating to each c_0 the highest probability (over all $c_1 \in \mathbb{C}$) for the template system to have bounded critical orbit. In particular, we considered the locus of $c_0 \in \mathbb{C}$ for which the peak value in the corresponding hybrid

set attains its highest possible value of 1. In other words, we searched for all “correct” maps f_{c_0} for which there exist *some* errors f_{c_1} that don’t affect sustainability of the system’s evolution initiated at rest, irrespective of the time of occurrence of these errors along the iteration. This locus is, of course, a subset of the traditional Mandelbrot set, which warrants the same bounded critical orbit property for the system in absence of error.

We then investigated how these results change when imposing the more restrictive condition that all critical points along the template iteration be bounded. We called the parameter loci obtained by this variation of the definition: multi-critical Mandelbrot sets. As shown by standard theorems in non-autonomous dynamics, the multi-critical Mandelbrot set for a fixed template iteration is equivalent with the Julia set connectedness locus. Hence, when the system is operating within the parameter range of the multi-critical Mandelbrot set, the resting state is surrounded by a connected region formed of all bounded initial conditions, so that the system can be perturbed continuously from rest into all its sustainable initial states.

Finally, we defined the multi-Mandelbrot set as the parameter locus in \mathbb{C}^2 of all (c_0, c_1) which render the critical orbit bounded when iterated in any random order. This is a 4-dimensional locus, which may be hard to visualize per se. One way to represent it is to plot 2-dimensional slices obtained by fixing one of the two complex parameters (say, c_0), to obtain a collection of complex subsets corresponding precisely to the dark red hybrid plateaux illustrated in the panels of Figure 4. Another way to represent the multi-Mandelbrot set is via 3-dimensional slices obtained by fixing one parameter and some aspect of the second parameter, such as its modulus, or its real/imaginary part (as done in Figure 6). The multi-Mandelbrot set represents the set of all map pairs which produce a bounded critical orbit under all possible template iterations. In the context of applications, this represents all combinations of “good” and “erroneous” transformations which can be iterated in any template order while retaining a sustainable evolution of the critical set.

We noticed that the multi-Mandelbrot set is the same for both definitions. This is therefore a very desirable parameter range. First, if one thinks of c_0 as the correct map and of c_1 as its perturbation, or error, having a pair (c_0, c_1) within the multi-Mandelbrot set guarantees sustainability of the resting system, independently of the frequency and timing of the errors along the template iteration. Second, this also implies sustainability if the system resets to rest at any point along the iteration.

5.2 Future work

This study represents only a first step in establishing and exploring significant questions for template iterations, in understanding their connection (similarities and differences) to the classical theory of single map iterations, as well as with exiting more general work in non-autonomous dynamics.

Our future work will focus on approaching analytically specific conjectures proposed in this paper. For example, one aspect which we have not pursued in this paper is the change in the shape and boundary of hybrid Mandelbrot sets \mathcal{M}_{c_0} as c_0 traverses different level sets of the contour set. Figure 4 suggests that hybrid sets have increased fractal behavior when $0 < \Pi_2(\mathcal{M}_{c_0}) < 1$, that is when c_0 corresponds to the transitional colors of the contour set (not inside the central plateau or in the outside blue region). While this is intuitively not surprising, we would like to investigate the idea further, both computationally and analytically. A lot of theoretical work remains to be done, and exploring these questions may require a combination of methods from traditional and non-autonomous iterations.

Part of our future work is also aimed at understanding the significance of our results in the context of applications to the life sciences. In particular, we have been considering the potential of using this theoretical framework to study natural iteration mechanisms, such as DNA replication. When a cell divides, it has to copy and transmit the exact same sequence of billions of nucleotides to its daughter cells. While most DNA is typically copied with high faithfulness, errors are a natural

part of the process, and sometimes escape repair mechanisms, so that a mutated cell will end up being used as a template for the next replication iteration, with the possibility to lead to substantial, accumulated changes in the structure of later daughter cells. On one hand, accumulating mutations can lead to pathologies like cancer. On the other hand, perfect replication would lead to no genetic variation. Organisms may have to construct successful mechanisms that optimize between these two ends. In our previous work [12], we have suggested that random iterations may be appropriate to study how the size and timing of these mutations affect cells in the long term. Our current work lays the grounds for contextualizing these questions within our mathematical framework.

Acknowledgements

The work on this project was supported by SUNY New Paltz, via the Research Scholarship and Creative Activities Program, as well as the Research and Creative Projects Awards Program.

References

- [1] Gaston Julia. Memoire sur l’iteration des fonctions rationnelles. *Journal de mathématiques pures et appliquées*, pages 47–246, 1918.
- [2] Pierre Fatou. Sur les équations fonctionnelles. *Bulletin de la société mathématique de France*, 48:33–94, 1920.
- [3] Bodil Branner and John H Hubbard. The iteration of cubic polynomials part ii: patterns and parapatterns. *Acta mathematica*, 169(1):229–325, 1992.
- [4] WeiYuan Qiu and YongCheng Yin. Proof of the branner-hubbard conjecture on cantor julia sets. *Science in China Series A: Mathematics*, 52(1):45–65, 2009.
- [5] Lennart Carleson and Theodore W Gamelin. *Complex dynamics*, volume 69. Springer Science & Business Media, 1993.
- [6] Robert L Devaney and Daniel M Look. A criterion for sierpinski curve julia sets. In *Topology Proceedings*, volume 30, pages 163–179, 2006.
- [7] John Erik Fornæss and Nessim Sibony. Random iterations of rational functions. *Ergodic Theory and Dynamical Systems*, 11(04):687–708, 1991.
- [8] Mark Comerford and Todd Woodard. Preservation of external rays in non-autonomous iteration. *Journal of Difference Equations and Applications*, 19(4):585–604, 2013.
- [9] Mark Comerford. Hyperbolic non-autonomous julia sets. *Ergodic Theory and Dynamical Systems*, 26(02):353–377, 2006.
- [10] Hiroki Sumi. Random complex dynamics and semigroups of holomorphic maps. *Proceedings of the London Mathematical Society*, page pdq013, 2010.
- [11] Marius-F Danca, M Romera, and G Pastor. Alternated julia sets and connectivity properties. *International Journal of Bifurcation and Chaos*, 19(06):2123–2129, 2009.
- [12] Anca Rădulescu and Ariel Pignatelli. Symbolic template iterations of complex quadratic maps. *Nonlinear Dynamics*, pages 1–18, 2015.
- [13] Bodil Branner. The Mandelbrot set. In *Proc. Symp. Appl. Math*, volume 39, pages 75–105, 1989.

- [14] John Milnor. Dynamics in one complex variable: Introductory lectures. *arXiv preprint math/9201272*, 1990.
- [15] Hiroki Sumi. Dynamics of postcritically bounded polynomial semigroups I: Connected components of the Julia sets. *Discrete and Continuous Dynamical Systems (DCDS-A)*, 29(3): 1205-1244, 2011.